Experimental Demonstration of Instrument-Specific Quantum Memory Effects and Non-Markovian Process Recovery for Common-Cause Processes

Yu Guo,[1,2,*] Philip Taranto,[3,4,*,§] Bi-Heng Liu,[1,2,†] Xiao-Min Hu,[1,2] Yun-Feng Huang,[1,2] Chuan-Feng Li,[1,2,‡] and Guang-Can Guo[1,2]

[1]*CAS Key Laboratory of Quantum Information, University of Science and Technology of China, Hefei 230026, People's Republic of China*

[2]*CAS Center for Excellence in Quantum Information and Quantum Physics, University of Science and Technology of China, Hefei 230026, People's Republic of China*

[3]*Institute for Quantum Optics and Quantum Information, Austrian Academy of Sciences, Boltzmanngasse 3, 1090 Vienna, Austria*

[4]*Vienna Center for Quantum Science and Technology, Atominstitut, Technische Universität Wien, 1020 Vienna, Austria*

(Received 16 June 2020; accepted 12 April 2021; published 9 June 2021)

The duration, strength, and structure of memory effects are crucial properties of physical evolution. Because of the invasive nature of quantum measurement, such properties must be defined with respect to the probing instruments employed. Here, using a photonic platform, we experimentally demonstrate this necessity via two paradigmatic processes: future-history correlations in the first process can be erased by an intermediate quantum measurement; for the second process, a noisy classical measurement blocks the effect of history. We then apply memory truncation techniques to recover an efficient description that approximates expectation values for multitime observables. Our proof-of-principle analysis paves the way for experiments concerning more general non-Markovian quantum processes and highlights where standard open systems techniques break down.

DOI: 10.1103/PhysRevLett.126.230401

Introduction.—Memory effects are ubiquitous in nature [1], including disease spreading [2], biochemical processes [3–5], and optical fiber transmission [6]. Characterizing stochastic processes with memory is difficult because past events can impact the future, so long-term history must be recorded for accurate prediction. This necessitates developing memory truncation techniques for efficient approximation.

Stochastic processes arise from the inability to track all relevant degrees of freedom, which partitions the Universe into an accessible "system" and an inaccessible "environment," leading to open dynamics. A classical stochastic process on discrete times $\{t_1, \ldots, t_n\}$ is characterized by the n-point joint probability distribution over event sequences, $\mathbb{P}_n(x_1, t_1; \cdots; x_n, t_n)$. For a process with approximately finite-length memory, this distribution conditionally factors over any length-ℓ sequence of memory events $\{x_{k+1}, \ldots, x_{k+\ell}\}$, with small error. This error is quantified by the conditional mutual information between the history $\{x_1, \ldots, x_k\}$ and future $\{x_{k+\ell+1}, \ldots, x_n\}$ events given the memory, which bounds the prediction accuracy when the history is truncated.

A key assumption here is that measurements do not affect the system. When invasive measurements are permitted in classical theory, such as in causal modeling [7], a joint probability distribution no longer describes the process [8]. Quantum theory is similar; however, here one cannot assume that noninvasive measurements could be made *in principle* [9], obfuscating the line between "process" and "observer" [10,11]. Many descriptions of open quantum dynamics have thus been restricted to two-time considerations [12,13], where an operational picture of correlations between preparations and measurements arises via the dynamical map formalism [14]. However, such approaches necessarily overlook multitime correlations; these methods provide *witnesses* of memory, but are insufficient to determine its presence [15–18] or properties [19–24].

These issues have hindered the precise formulation of quantum stochastic processes and led to a "zoo" of definitions for memorylessness [16], some of which are contradictory [25–27]. Recently, the process tensor formalism [17–19], which captures *all* detectable multitime correlations, has been developed (see also Refs. [28–37]). This framework separates the controllable impact on system dynamics due to an agent from the uncontrollable environmental influence: the former is described by quantum instruments, which capture the postmeasurement states for each (probabilistically occurring) outcome; the process comprises the latter. This provides a consistent operational description of multitime quantum stochastic processes that generalizes and unifies open quantum dynamics [19]. The process tensor correctly generalizes classical stochastic processes via a generalized Kolmogorov extension theorem [8], and all memory properties such as Markovianity (memorylessness) and Markov order (finite-length memory) can be rigorously defined and recover classical definitions [18–22,38].

It was recently shown that there do not exist non-Markovian processes with finite-length memory for all instruments (although for any particular instrument, the memory length can be finite); thus operational descriptions of memory length must specify the probing instruments [20–22]. In this Letter, we experimentally demonstrate this instrument-specific nature of quantum memory via two three-time quantum processes on a photonic platform. Both processes are non-Markovian; however, by performing specific intermediate instruments, we show that future-history correlations can be deterministically erased, exemplifying finite-length memory for instruments. We then use memory truncation techniques developed in Ref. [22] to approximate non-Markovian processes with small memory strength and show this *recovered* description to accurately predict multitime expectation values. Our results provide the first demonstration of multitime quantum memory effects beyond the two-time setting [39–41]; while our proof-of-principle experiment focuses on "common-cause processes" [42,43], in which correlations arise from an initial state, the methods employed are readily adaptable to the analysis of more general non-Markovian processes.

Multitime quantum processes.—See the Supplemental Material [44] for an introduction to the process tensor; here, we outline its key features. The process tensor is a linear mapping from sequences of quantum instruments—collections of completely positive (CP) maps that sum to a completely positive, trace-preserving (TP) map [28]—to the joint probability of their realization. Just as a density operator contains all necessary information to compute the probability of any measurement event via the Born rule, the process tensor encapsulates all information required to calculate the probability of realizing any sequence of events through a generalized Born rule [47]. Any process tensor that decomposes into independent channels between time steps is Markovian; by considering the distance to the nearest Markovian process, one can quantify the memory [18]. The process tensor can be tomographically reconstructed, constituting an operational description of quantum stochastic processes [48]. Conversely, any operator satisfying generalized notions of complete positivity and normalization, and a causality condition ensuring temporal order, represents some underlying open quantum dynamics [19,32], i.e., can be dilated to a joint system-environment state evolving unitarily between times, with the environment finally discarded.

While it is straightforward to compute the process tensor from a dilation, i.e., an underlying system-environment model (which is nonunique), it is difficult to engineer processes with certain memory properties. This is because correlations play a dynamical role and it is often unclear how to best design them within practical constraints. Moreover, the output states of each measurement generally influence future dynamics, presenting another experimental difficulty. To circumvent these problems, we examine two processes of a similar type, depicted in Fig. 1: ones for which subsystems of an initially correlated state are fed out over time, with the output states discarded after each step. Such common-cause processes are a subset of general quantum processes that are amenable to current laboratory methods, as all correlations are encoded in the initial state. In particular, we examine the memory effects of two processes over three time steps, which is the minimal setting for analyzing multitime phenomena. We denote the initial 3-qubit state of Process 1 by $\lambda_{\mathrm{ABC}} \in \mathsf{BL}(\mathcal{H}^2 \otimes \mathcal{H}^2 \otimes \mathcal{H}^2)$ and the corresponding process tensor by Λ_{ABC}. Process 2 is from Appendix E of Ref. [21]; we denote its initial qubit-qutrit-qubit state by $\omega_{\mathrm{ABC}} \in \mathsf{BL}(\mathcal{H}^2 \otimes \mathcal{H}^3 \otimes \mathcal{H}^2)$ and its process tensor by Ω_{ABC}, note BL denotes the set of bounded linear operators. Both common-cause states exhibit complicated correlations with nontrivial off-diagonal elements (see Supplemental Material [44]). The distinct memory effects displayed are due to the types of history-blocking instruments: for the former process, these are three-outcome qubit measurements with no classical analog, demonstrating a genuinely quantum effect; for the latter process, these are noisy classical measurements, highlighting how coarse graining can hide memory and positing Markovianity as an emergent phenomenon.

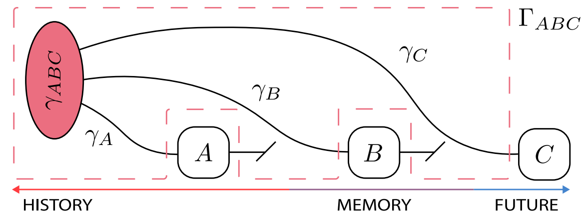

FIG. 1. Process schematic. Parts of an initial state γ_{ABC} are sent to Alice, Bob, and Charlie in a time-ordered fashion. Alice and Bob's outputs are discarded, corresponding to an identity matrix in the Choi representation, where each time step has two Hilbert spaces (input and output). The resulting process tensor is $\Gamma_{\mathrm{ABC}} = \gamma_{\mathrm{A}^i\mathrm{B}^i\mathrm{C}^i} \otimes \mathbb{1}_{\mathrm{A}^o\mathrm{B}^o}$.

Experimental setup.—The processes considered comprise an initially correlated state with parts sent out first to Alice (history), then to Bob (memory), and finally to Charlie (future), with each agent permitted freedom of choice and an optical delay line ensuring temporal order. The post measurement states of Alice and Bob are discarded. The initial correlations encode the common-cause memory effects of the process [35,43,49,50]; thus, state preparation is crucial to our experiment. We use a linear photonic system (see Fig. 2). The "source" prepares tripartite states encoded in path and polarization degrees of freedom of photon pairs. Although various techniques to construct multipartite states exist [51–54], many require distinct systems. We opt for a hybrid approach that encodes information in various degrees of freedom. This choice is motivated by the development of linear optical methods [55–57], which provide a high-fidelity and postselection-free approach. The second critical element to our

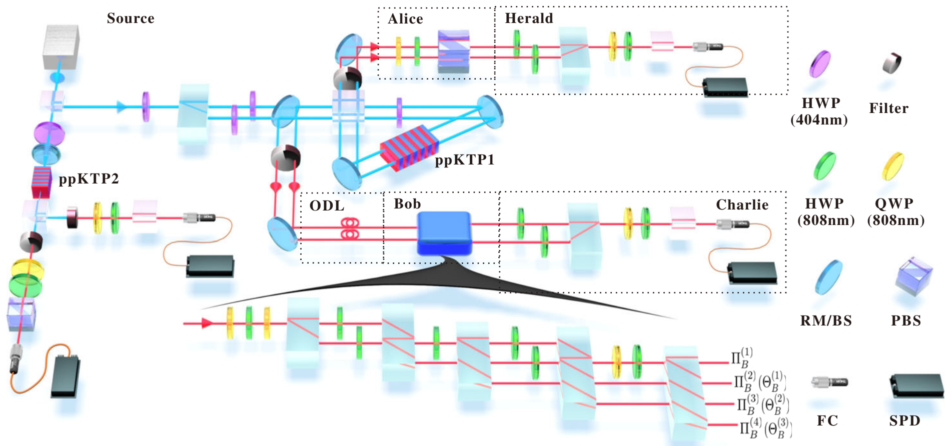

FIG. 2. Experimental setup. An entangled photon pair is generated via spontaneous parametric down-conversion (SPDC) at ppKTP1 in a Sagnac interferometer pumped by a 404 nm laser. For Process 1, the polarization acts as history and memory and path qubits as future and herald. For Process 2, an additional SPDC at ppKTP2 constructs a third level. Conditional Alice-Charlie correlations for each of Bob's outcomes encode memory effects. Inset: Bob's measurement apparatus [58,59]. Abbreviations: ODL—optical delay line; HWP—half-wave plate; QWP—quarter-wave plate; RM/BS—reflection mirror/beam splitter; PBS—polarizing beam splitter; FC—fiber coupler; SPD—single photon detector; and ppKTP—periodically poled potassium titanyl phosphate.

experiment is implementing positive operator-valued measurements (POVMs). We use a discrete-time quantum walk protocol [58,59] (see Supplemental Material [44]).

Results.—Non-Markovianity: For both processes $\Gamma_{\mathrm{ABC}} \in \{\Lambda_{\mathrm{ABC}}, \Omega_{\mathrm{ABC}}\}$, the non-Markovianity is the distance to its nearest Markovian counterpart

$$\mathcal{N} := \min_{\Gamma^{\mathrm{Markov}}_{\mathrm{ABC}}} \mathcal{D}(\Gamma_{\mathrm{ABC}} \| \Gamma^{\mathrm{Markov}}_{\mathrm{ABC}}). \tag{1}$$

Choosing the quantum relative entropy $S(X\|Y) := tr[X(\log X - \log Y)]$ as the distance [60], the minimum is achieved by the process constructed from its marginals [61], $\gamma_X := tr_{YZ}[\gamma_{XYZ}]$, i.e., $\Gamma^{\mathrm{Markov}}_{\mathrm{ABC}} = \gamma_{\mathrm{A}^i} \otimes \mathbb{1}_{\mathrm{A}^o} \otimes \gamma_{\mathrm{B}^i} \otimes \mathbb{1}_{\mathrm{B}^o} \otimes \gamma_{\mathrm{C}^i}$. The following results hold for any *CP*-contractive (pseudo-)distance; the choice of the relative entropy bypasses optimization over Markovian processes and has an operational interpretation: $P_{\mathrm{confusion}} := \exp(-n\mathcal{N})$ is the probability of confusing the process with a promised Markovian one after n measurements [18,62]. In the Supplemental Material [44], we present the experimental tomographic data based on temporally ordered measurements performed on the common-cause state at the three laboratories for both processes. For Λ_{ABC}, the non-Markovianity is 0.285 ± 0.004 and for Ω_{ABC} it is 0.458 ± 0.004, with theoretical predictions 0.329 and 0.5, respectively.

Both processes are, however, *CP* divisible, meaning all two-point dynamics can be described by composition of (fictitious) CPTP channels, i.e., $\Lambda_{\mathrm{A}^o\mathrm{C}^i} = \Lambda_{\mathrm{B}^o\mathrm{C}^i} \circ \Lambda_{\mathrm{A}^o\mathrm{B}^i}$. As the output states discarded, one has $\Lambda_{\mathrm{A}^o\mathrm{B}^i} = \mathbb{1}_{\mathrm{A}^o} \otimes \gamma_{\mathrm{B}^i}$ and $\Lambda_{\mathrm{B}^o\mathrm{C}^i} = \mathbb{1}_{\mathrm{B}^o} \otimes \gamma_{\mathrm{C}^i}$; similarly, any common-cause process is *CP* divisible, which is often used as a proxy for quantum Markovianity [12,13]. Nonetheless, *CP* divisibility only considers two-point correlations; thus, while it can witness non-Markovianity, it is insufficient to conclude that a process is Markovian, which requires checking multitime conditions [24]. For more general non-Markovian quantum processes than the common-cause ones considered here, all such two-point techniques necessarily fail, whereas the process tensor formalism is tailor-made for their analysis.

Markov order: We now demonstrate that both processes—although non-Markovian—have finite Markov order for particular instruments. The Markov order is the minimum number of times over which an agent must act to block history-future correlations [63]. Both processes have Markov order 1 [64], meaning that Bob can apply an instrument $\mathcal{J}_{\mathrm{B}} = \{\mathsf{O}^{(x)}_{\mathrm{B}}\}$ such that, for each event, Alice and Charlie are conditionally independent

$$tr_{\mathrm{B}}[\mathsf{O}^{(x)\mathsf{T}}_{\mathrm{B}} \Gamma_{\mathrm{ABC}}] = \Gamma^{(x)}_{\mathrm{A}} \otimes \Gamma^{(x)}_{\mathrm{C}}. \tag{2}$$

By performing $\mathcal{J}_{\mathrm{B}}$, Bob deterministically erases the memory. Deviation from Eq. (2), i.e., a correlated conditional process for any event of an instrument, evidences longer memory with respect to said instrument.

For Process 1, Λ_{ABC}, the history-blocking instrument is a POVM $\Theta_{\mathrm{B}} = \{\Theta^{(x)}_{\mathrm{B}}\}$ comprising

$$\Theta^{(1)}_{\mathrm{B}} = \frac{\sqrt{2}}{1+\sqrt{2}} |1\rangle\langle 1|,$$
$$\Theta^{(2)}_{\mathrm{B}} = \frac{\sqrt{2}}{2(1+\sqrt{2})} (|0\rangle - |1\rangle)(\langle 0| - \langle 1|),$$
$$\Theta^{(3)}_{\mathrm{B}} = \mathbb{1} - \Theta^{(1)}_{\mathrm{B}} - \Theta^{(2)}_{\mathrm{B}}. \tag{3}$$

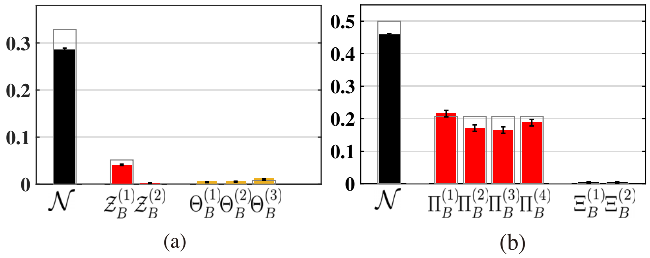

FIG. 3. Non-Markovianity and memory strength of (a) Process 1 and (b) Process 2. Experimental results for the non-Markovianity $\mathcal{N}$ (black, left), the (nonvanishing) memory strength for (a) the computational-basis measurement $\mathcal{Z}_\mathrm{B} = \{\mathcal{Z}_\mathrm{B}^{(x)}\}$, and (b) POVM $\Pi_\mathrm{B} = \{\Pi_\mathrm{B}^{(x)}\}$ (red, middle) [Eq. (4)], and the (vanishing) memory strength for (a) the POVM $\Theta_\mathrm{B} = \{\Theta_\mathrm{B}^{(x)}\}$ [Eq. (3)] and (b) noisy measurement $\Xi_\mathrm{B} = \{\Xi_\mathrm{B}^{(x)}\}$ (yellow, right). Each bar shows the mutual information between Alice and Charlie, conditioned on Bob's event. Gray edges show theoretical predictions.

Figure 3(a) depicts the mutual information, $S_\mathrm{AC} \coloneqq S_\mathrm{A} + S_\mathrm{C} - S_\mathrm{AC}$, with S_X the von Neumann entropy, of the conditional processes. The memory strength for each event of Θ_B is $0.0042 \pm 0.0010, 0.0053 \pm 0.0010$, and 0.0098 ± 0.0014, signifying negligible Alice-Charlie correlations, with an average memory strength of $(6.3 \pm 1.1) \times 10^{-3}$. Conversely, if Bob measures in the computational basis $\mathcal{Z}_\mathrm{B} = \{|0\rangle\langle 0|, |1\rangle\langle 1|\}$ then Alice and Charlie's conditional processes are correlated; for instance, the first event of $\mathcal{Z}_\mathrm{B}$ has memory strength 0.0410 ± 0.0015 [see middle bars in Fig. 3(a)]. The fact that this history-blocking instrument comprises a three-outcome POVM, which has no classical analog, signifies that the approximate recovery we construct below represents a genuinely quantum approximation, in the sense that no recovery with respect to projective measurements would be as accurate or versatile. Nonetheless, for this process, certain projective measurements can render Alice and Charlie approximately conditionally independent (see Supplemental Material [44]). We conjecture that in higher dimensions, there exist processes for which *no* set of orthogonal projectors block the history, but certain POVMs do.

Process 2, Ω_ABC, highlights how coarse graining can block memory. If Bob performs a *noisy* classical measurement $\Xi_\mathrm{B} = \{\Xi_\mathrm{B}^{(x)}\} = \{\mathbb{1}_{01}, |2\rangle\langle 2|\}$ that cannot distinguish events on the first two levels of his qutrit, the process has Markov order 1, depicted by the rightmost bars in Fig. 3(b), which vanish for each event (the experimental value is 0.004 ± 0.002). On the other hand, if Bob performs a three-level measurement that resolves events in the first two levels, then Alice's and Charlie's conditional processes can be correlated. For instance, consider the POVM $\Pi_\mathrm{B} = \{\Pi_\mathrm{B}^{(x)}\}$,

$$\Pi_\mathrm{B}^{(x)} = \frac{1}{4}\left(\mathbb{1} + \frac{1}{\sqrt{3}}\sum_j c_j^{(x)}\sigma_j\right), \tag{4}$$

where $\{\mathbb{1}, \sigma_X, \sigma_Y, \sigma_Z\}$ are Pauli matrices with coefficients $\{c^{(x)}\} = \{(1,1,1), (1,-1,-1), (-1,1,-1), (-1,-1,1)\}$. The measurement events, respectively, have memory strength 0.216 ± 0.001, 0.171 ± 0.0009, 0.165 ± 0.001, and 0.188 ± 0.0009, as shown by the middle bars in Fig. 3(b) (see Supplemental Material [44]). These memory effects are close to maximal and one expects that some memory will be present for generic three-level POVMs; however, it is also likely that there exist fine-grained measurements that approximately render Alice and Charlie uncorrelated for each outcome. Our results are relevant toward understanding Markovianity as a consequence of coarse graining.

Knowledge of any approximately history-blocking instrument allows one to "recover" an efficient and accurate description, as we now demonstrate.

Efficient recovery: In general, the conditional processes for an instrument applied by Bob are correlated. Aggregating the mutual information of the conditional processes to the instrument level quantifies the memory strength in an instrument-specific manner [22]. One can then upper bound the difference between a class of multi-time expectation values calculated with the actual process (i.e., with common-cause state γ_ABC) versus a recovered process (see below), which efficiently approximates the true one by discarding future-history correlations (see Supplemental Material [44]).

Since both processes have vanishing memory strength for some instrument, one can reconstruct an accurate such recovered processes. For common-cause processes, the reconstruction with respect to Bob's history-blocking measurement $\mathcal{J}_{\mathrm{B}^i} = \{\mathsf{O}_{\mathrm{B}^i}^{(x)}\}$ has the common-cause state

$$\underline{\gamma}_\mathrm{ABC}^{\mathcal{J}_\mathrm{B}} = \sum_x \gamma_{\mathrm{A}^i}^{(x)} \otimes \Delta_{\mathrm{B}^i}^{(x)} \otimes \gamma_{\mathrm{C}^i}^{(x)}, \tag{5}$$

where $\{\gamma_{\mathrm{A}^i}^{(x)}, \gamma_{\mathrm{C}^i}^{(x)}\}$ are the marginals of Alice and Charlie for each outcome Bob yields and $\{\Delta_{\mathrm{B}^i}^{(x)}\}$ satisfies $tr[\Delta_{\mathrm{B}^i}^{(x)} \mathsf{O}_{\mathrm{B}^i}^{(y)\mathrm{T}}] = \delta_{xy}$ [65]. We tomographically reconstruct the marginals from local measurements of Alice and Charlie for Bob's outcomes. The approximate process $\underline{\Gamma}_\mathrm{ABC}^{\mathcal{J}_\mathrm{B}} = \underline{\gamma}_\mathrm{ABC}^{\mathcal{J}_\mathrm{B}} \otimes \mathbb{1}_{\mathrm{A}^o\mathrm{B}^o}$ accurately predicts expectation values for any observable of the form $C_\mathrm{ABC} = \sum_y c_y \mathsf{X}_\mathrm{ABC}^{(y)}$ where $\mathsf{X}^{(y)} = \sum_x \mathsf{E}_\mathrm{AC}^{(x,y)} \otimes \mathsf{O}_\mathrm{B}^{(x)}$, with arbitrary $\mathsf{E}_\mathrm{AC}^{(x,y)}$; this ensures that Bob's observable is in the span of the original instrument, as required for the recovered process to make sensible predictions [22].

In Fig. 4 we consider projective measurements for Alice and Charlie, with Bob performing any nonselective measurement. This choice permits arbitrary product Alice-Charlie observables; more complicated temporally correlated observables would require higher levels of control that are not presently available. We scan the parameter space

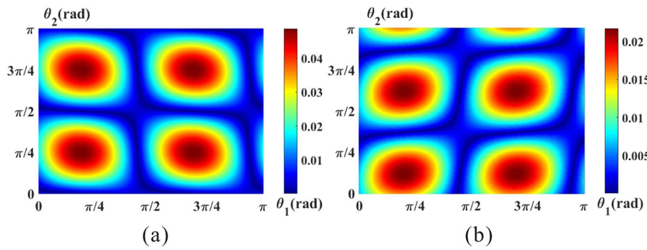

FIG. 4. Multitime expectations for (a) Process 1 and (b) Process 2. Alice and Charlie project onto orthogonal states $\{|\phi\rangle = \cos\theta_1|0\rangle + e^{i\phi}\sin\theta_1|1\rangle, |\phi\rangle^\perp = \sin\theta_1|0\rangle - e^{-i\phi}\cos\theta_1|1\rangle\}$ and $\{|\psi\rangle = \cos\theta_2|0\rangle + e^{i\psi}\sin\theta_2|1\rangle, |\psi\rangle^\perp = \sin\theta_2|0\rangle - e^{-i\psi}\cos\theta_2|1\rangle\}$, respectively, and Bob performs any nonselective measurement. The difference of expectation values via the recovered and true process is plotted for fixed phase (a) $\phi = 0$ and $\psi = 0$ and (b) $\phi = 1.920\pi$ and $\psi = \pi$.

and compare the expectation values calculated from the recovered and true process, finding maximum deviations of 0.048 and 0.022 for processes 1 and 2, respectively; the maximum difference for an arbitrary process is 1, highlighting the approximation accuracy. Finally, the memory strength with respect to Bob's instrument $\mathcal{J}_B$ bounds the inaccuracy of approximating *any* observable of the form below Eq. (5); this includes, e.g., correlated Alice-Charlie observables [22]. Calculating the memory strength for Θ_B and Ξ_B for the two processes, respectively, gives a bound of 0.450 ± 0.017 and 0.348 ± 0.015.

Conclusions and outlook.—In this Letter, we have demonstrated the instrument-specific nature of quantum memory. Our experiment provides the first report of finite quantum Markov order for non-Markovian common-cause processes, i.e., the ability to erase future-history correlations, stored in a correlated initial state, via a specific instrument. This has implications for the approximation of quantum processes with memory, which we highlighted by reconstructing the recovered process that disregards negligible correlations and showing this to accurately predict multitime expectation values. Such memory truncation techniques are pivotal to efficiently characterizing near-term quantum devices.

Our Letter opens some important avenues: we have posed the question of whether there exist processes for which no orthogonal measurement blocks the history, but certain POVMs do, and that concerning the emergence of Markovianity via coarse graining. Analyzing the relative volumes of measurement space that lead to finite Markov order, as well as the tightness of the bounds, is warranted to develop more robust approximations.

The common-cause processes analyzed here are an important class of non-Markovian processes; in particular, they display global memory properties that could not be characterized from standard two-point measurement techniques. On the other hand, all correlations arising from such processes can be computed from measurements on the initial common-cause state, as the postmeasurement states play no role, making them more amenable to current experimental platforms. By phrasing the analysis of such memory effects in the operational process tensor formalism and highlighting where other techniques would fail, our Letter provides a starting point for the analysis of more general processes (e.g., those for which postmeasurement states play a role). Such experiments will require high levels of quantum control and the ability to implement multi-input to multi-output gates. As such technical challenges are overcome, a holistic analysis of multitime quantum memory effects will become possible.

We thank Kavan Modi for discussions. This work was supported by the National Key Research and Development Program of China (No. 2017YFA0304100, No. 2016YFA0301300, and No. 2016YFA0301700), NSFC (No. 11774335, No. 11734015, No. 11874345, No. 11821404, No. 11904357), the Key Research Program of Frontier Sciences, CAS (No. QYZDY-SSW-SLH003), Science Foundation of the CAS (No. ZDRW-XH-2019-1), the Fundamental Research Funds for the Central Universities, USTC Tang Scholarship, Science and Technological Fund of Anhui Province for Outstanding Youth (2008085J02), and Anhui Initiative in Quantum Information Technologies (No. AHY020100, No. AHY060300). P. T. was supported by the Austrian Science Fund (FWF) START Project (No. Y879-N27).

[*] Y. G. and P. T. contributed equally to this work.
[†] bhliu@ustc.edu.cn
[‡] cfli@ustc.edu.cn
[§] philip.taranto@oeaw.ac.at

[1] N. Van Kampen, *Stochastic Processes in Physics and Chemistry* (Elsevier, New York, 2011).
[2] A. Pimenov, T. C. Kelly, A. Korobeinikov, M. J. A. O'Callaghan, A. V. Pokrovskii, and D. Rachinskii, Math. Model. Nat. Phenom. **7**, 204 (2012).
[3] N. Lambert, Y.-N. Chen, Y.-C. Cheng, C.-M. Li, G.-Y. Chen, and F. Nori, Nat. Phys. **9**, 10 (2013).
[4] G. D. Scholes, G. R. Fleming, L. X. Chen, A. Aspuru-Guzik, A. Buchleitner, D. F. Coker, G. S. Engel, R. van Grondelle, A. Ishizaki, D. M. Jonas, J. S. Lundeen, J. K. McCusker, S. Mukamel, J. P. Ogilvie, A. Olaya-Castro, M. A. Ratner, F. C. Spano, K. B. Whaley, and X. Zhu, Nature (London) **543**, 647 (2017).
[5] L. Wang, M. A. Allodi, and G. S. Engel, Nat. Rev. Chem. **3**, 477 (2019).
[6] K. Banaszek, A. Dragan, W. Wasilewski, and C. Radzewicz, Phys. Rev. Lett. **92**, 257901 (2004).
[7] J. Pearl, *Causality* (Oxford University Press, New York, 2000).
[8] S. Milz, F. Sakuldee, F. A. Pollock, and K. Modi, Quantum **4**, 255 (2020).
[9] C. Piron, Erkenntnis **16**, 397 (1981).
[10] K. Modi, Open Syst. Inf. Dyn. **18**, 253 (2011).
[11] K. Modi, Sci. Rep. **2**, 581 (2012).

[12] Á. Rivas, S. F. Huelga, and M. B. Plenio, Rep. Prog. Phys. **77**, 094001 (2014).

[13] H.-P. Breuer, E.-M. Laine, J. Piilo, and B. Vacchini, Rev. Mod. Phys. **88**, 021002 (2016).

[14] E. C. G. Sudarshan, P. M. Mathews, and J. Rau, Phys. Rev. **121**, 920 (1961).

[15] I. de Vega and D. Alonso, Rev. Mod. Phys. **89**, 015001 (2017).

[16] L. Li, M. J. Hall, and H. M. Wiseman, Phys. Rep. **759**, 1 (2018).

[17] S. Milz, F. A. Pollock, and K. Modi, Open Syst. Inf. Dyn. **24**, 1740016 (2017).

[18] F. A. Pollock, C. Rodríguez-Rosario, T. Frauenheim, M. Paternostro, and K. Modi, Phys. Rev. Lett. **120**, 040405 (2018).

[19] F. A. Pollock, C. Rodríguez-Rosario, T. Frauenheim, M. Paternostro, and K. Modi, Phys. Rev. A **97**, 012127 (2018).

[20] P. Taranto, F. A. Pollock, S. Milz, M. Tomamichel, and K. Modi, Phys. Rev. Lett. **122**, 140401 (2019).

[21] P. Taranto, S. Milz, F. A. Pollock, and K. Modi, Phys. Rev. A **99**, 042108 (2019).

[22] P. Taranto, F. A. Pollock, and K. Modi, arXiv:1907.12583.

[23] P. Taranto, Int. J. Quantum. Inform. **18**, 1941002 (2020).

[24] S. Milz, M. S. Kim, F. A. Pollock, and K. Modi, Phys. Rev. Lett. **123**, 040401 (2019).

[25] L. Mazzola, E.-M. Laine, H.-P. Breuer, S. Maniscalco, and J. Piilo, Phys. Rev. A **81**, 062120 (2010).

[26] P. Haikka, J. D. Cresser, and S. Maniscalco, Phys. Rev. A **83**, 012112 (2011).

[27] D. Chruściński, A. Kossakowski, and A. Rivas, Phys. Rev. A **83**, 052128 (2011).

[28] G. Lindblad, Commun. Math. Phys. **65**, 281 (1979).

[29] L. Accardi, A. Frigerio, and J. T. Lewis, Publ. RIMS **18**, 97 (1982).

[30] D. Kretschmann and R. F. Werner, Phys. Rev. A **72**, 062323 (2005).

[31] G. Chiribella, G. M. D'Ariano, and P. Perinotti, Phys. Rev. Lett. **101**, 060401 (2008).

[32] G. Chiribella, G. M. D'Ariano, and P. Perinotti, Phys. Rev. A **80**, 022339 (2009).

[33] O. Oreshkov, F. Costa, and Č. Brukner, Nat. Commun. **3**, 1092 (2012).

[34] O. Oreshkov and C. Giarmatzi, New J. Phys. **18**, 093020 (2016).

[35] F. Costa and S. Shrapnel, New J. Phys. **18**, 063032 (2016).

[36] L. Hardy, Phil. Trans. R. Soc. A **370**, 3385 (2012).

[37] L. Hardy, arXiv:1608.06940.

[38] S. Milz, D. Egloff, P. Taranto, T. Theurer, M. B. Plenio, A. Smirne, and S. F. Huelga, Phys. Rev. X **10**, 041049 (2020).

[39] B.-H. Liu, L. Li, Y.-F. Huang, C.-F. Li, G.-C. Guo, E.-M. Laine, H.-P. Breuer, and J. Piilo, Nat. Phys. **7**, 931 (2011).

[40] A. Chiuri, C. Greganti, L. Mazzola, M. Paternostro, and P. Mataloni, Sci. Rep. **2**, 968 (2012).

[41] Z.-D. Liu, H. Lyyra, Y.-N. Sun, B.-H. Liu, C.-F. Li, G.-C. Guo, S. Maniscalco, and J. Piilo, Nat. Commun. **9**, 3453 (2018).

[42] S. Milz, C. Spee, Z.-P. Xu, F. A. Pollock, K. Modi, and O. Gühne, arXiv:2011.09340.

[43] M. Nery, M. Túlio Quintino, P. A. Guérin, T. O. Maciel, and O. V. Reinaldo, arXiv:2101.11630.

[44] See Supplemental Material at http://link.aps.org/supplemental/10.1103/PhysRevLett.126.230401 for details about the process tensor formalism, processes constructed, experimental implementation, and analysis of results. This includes Refs. [45,46].

[45] X.-M. Hu, Y. Guo, B.-H. Liu, Y.-F. Huang, C.-F. Li, and G.-C. Guo, Sci. Adv. **4**, eaat9304 (2018).

[46] Y. Guo, S. Cheng, X. Hu, B.-H. Liu, E.-M. Huang, Y.-F. Huang, C.-F. Li, G.-C. Guo, and E. G. Cavalcanti, Phys. Rev. Lett. **123**, 170402 (2019).

[47] S. Shrapnel, F. Costa, and G. Milburn, New J. Phys. **20**, 053010 (2018).

[48] S. Milz, F. A. Pollock, and K. Modi, Phys. Rev. A **98**, 012108 (2018).

[49] M. Ringbauer and R. Chaves, Quantum **1**, 35 (2017).

[50] M. Ringbauer, F. Costa, M. E. Goggin, A. G. White, and A. Fedrizzi, npj Quantum Inf. **4**, 37 (2018).

[51] J.-W. Pan, Z.-B. Chen, C.-Y. Lu, H. Weinfurter, A. Zeilinger, and M. Żukowski, Rev. Mod. Phys. **84**, 777 (2012).

[52] S. Yokoyama, R. Ukai, S. C. Armstrong, C. Sornphiphatphong, T. Kaji, S. Suzuki, J.-i. Yoshikawa, H. Yonezawa, N. C. Menicucci, and A. Furusawa, Nat. Photonics **7**, 982 (2013).

[53] T. Monz, P. Schindler, J. T. Barreiro, M. Chwalla, D. Nigg, W. A. Coish, M. Harlander, W. Hänsel, M. Hennrich, and R. Blatt, Phys. Rev. Lett. **106**, 130506 (2011).

[54] M. Ansmann, H. Wang, R. C. Bialczak, M. Hofheinz, E. Lucero, M. Neeley, A. D. O'Connell, D. Sank, M. Weides, J. Wenner, A. N. Cleland, and J. M. Martinis, Nature (London) **461**, 504 (2009).

[55] S. Takeuchi, Phys. Rev. A **62**, 032301 (2000).

[56] Y. Zhang, F. S. Roux, T. Konrad, M. Agnew, J. Leach, and A. Forbes, Sci. Adv. **2**, e1501165 (2016).

[57] C. Reimer, S. Sciara, P. Roztocki, M. Islam, L. R. Cortés, Y. Zhang, B. Fischer, S. Loranger, R. Kashyap, A. Cino *et al.*, Nat. Phys. **15**, 148 (2019).

[58] P. Kurzyński and A. Wójcik, Phys. Rev. Lett. **110**, 200404 (2013).

[59] Y.-Y. Zhao, N.-K. Yu, P. Kurzyński, G.-Y. Xiang, C.-F. Li, and G.-C. Guo, Phys. Rev. A **91**, 042101 (2015).

[60] Since entropies are only well defined for normalized quantities, we calculate them on normalized process tensors in the Choi state representation, i.e., for $\hat{\Gamma} = \Gamma/tr[\Gamma]$, $S_X = -\hat{\Gamma}_X \log[\hat{\Gamma}_X]$.

[61] V. Vedral, Rev. Mod. Phys. **74**, 197 (2002).

[62] S. Milz and K. Modi, arXiv:2012.01894.

[63] Our methods apply to processes in which Bob could act multiple times between Alice and Charlie, capturing higher Markov order.

[64] For quantum processes, Markov order 1 does not necessarily coincide with Markovianity: quantum Markovianity means that if Bob performs an informationally complete measurement and independent repreparation, Charlie's state only depends upon Bob's repreparation, which is not the case here.

[65] Such a set of operators always exists for linearly independent measurement elements [66].

[66] K. Modi, C. A. Rodríguez-Rosario, and A. Aspuru-Guzik, Phys. Rev. A **86**, 064102 (2012).